Mathematical Biology and Bioinformatics
2015. V. 10. № 1. P. 164-177. doi: 10.17537/2015.10.164

========== **MATHEMATICAL MODELING** ==========

UDC: 519.8

Kinks behavior near the boundaries separating homogeneous regions of DNA

Grinevich A.A.*, Yakushevich L.V.

Institute of Cell Biophysics, Russian Academy of Sciences, Pushchino, Moscow Region, Russia

Abstract. In this paper we derive a new modification of the sine-Gordon equation that is suitable for simulation of angular oscillations of nitrous bases in a heterogeneous DNA. The equation is applied to study the behavior of nonlinear conformational waves – kinks – near the boundaries separating homogeneous regions in the DNA sequence.

Keywords: *mathematical modeling, sine-Gordon equation, the dynamics of DNA, kink trajectory.*

INTRODUCTION

When modeling the angular oscillations of nitrous bases in homogeneous DNA, researchers often use a simple sine-Gordon equation with constant coefficients [1–3] whose values are determined by the physical parameters of DNA: the moment of inertia of bases (I), the torsion rigidity of the sugar-phosphate backbone (K') and the coefficient of the interaction between the bases in pairs (V). When passing to the case of inhomogeneous DNA these coefficients are usually replaced by the functions which depend on the base sequence [4–7].

However, it turned out that the use of this simple approach for solving the problems associated with artificial heterogeneous sequence consisting of several homogeneous areas, in certain cases leads to contradictions [8]. Analysis of the reasons causing these contradictions, led us to the necessity to revise the original model and derive a new modification of the model equation [9]. In this paper we present a detailed derivation the new equation. We show that the new modification actually removes the above contradictions. We also apply the new equation to study of the behavior of nonlinear conformational waves – kinks – near the boundaries separating homogeneous regions of DNA.

MODEL EQUATION

To derive a new modification of the sine-Gordon equation that simulates the angular oscillations of the nitrous bases in heterogeneous DNA, let us use the mechanical analogue: the chain of coupled unequal pendulums oscillating in the gravitational the Earth field [10] (Fig. 1). In the mechanical analogue, the pendulums play the role of nitrous bases, the springs – the role of the sugar-phosphate chains, the gravitational field – the role of the field induced by the second DNA strand.

As a start, let us take the equation for angular oscillations of one (isolated) pendulum:

$$I\frac{d^2\phi}{dt^2}+V\sin\phi=0, \qquad (1)$$

*grin_aa@mail.ru

where $\phi(t)$ is the angular displacement of the pendulum, $I = mR^2$, $V = mgR$, m and R are the mass and length of the pendulum, g is the gravitational constant.

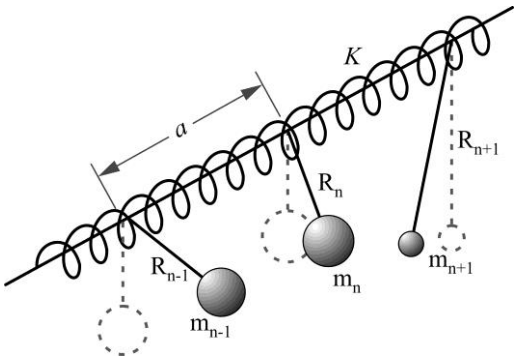

Fig. 1. Chain of pendulums.

Then transform equation (1) to the form:

$$mR\frac{d^2(R\phi)}{dt^2} + mgR\sin(\phi) = 0 \tag{2}$$

and divide all terms of equation (2) by R:

$$m\frac{d^2(R\phi)}{dt^2} + mg\sin(\phi) = 0\ . \tag{3}$$

After that let us pass from equation (3) obtained for the isolated pendulum, to the equation of oscillations of the n-th pendulum in the chain of coupled pendulums. For the purpose, we add two terms that imitate interaction with the neighboring pendulums:

$$m_n\frac{d^2(R_n\phi_n)}{dt^2} + m_n g\sin\phi_n + f_{left} - f_{right} = 0\ . \tag{4}$$

Here $f_{left} = K_{left}(R_n\phi_n - R_{n-1}\phi_{n-1})$ is the force acting on the n-th pendulum from the nearest neighbor to the left, $f_{right} = K_{right}(R_{n+1}\phi_{n+1} - R_n\phi_n)$ is the force acting on the n-th pendulum from the nearest neighbor to the right, K is the stiffness of springs. Hereinafter we assume that all springs in the mechanical analogue are identical:

$$K_{left} = K_{right} = K\ . \tag{5}$$

This corresponds to the situation which is really taking place in the DNA, where the role of the horizontal thread with springs plays the sugar-phosphate chain with a strictly regular structure. In contrast to the springs, the pendulums are not identical and have different mass m_n and length R_n (n = 1, 2,…, N).

Taking into account relations (5), we can rewrite equation (4) as:

$$m_n\frac{d^2(R_n\phi_n)}{dt^2} + m_n g\sin(\phi_n) + K(R_n\phi_n - R_{n-1}\phi_{n-1}) - K(R_{n+1}\phi_{n+1} - R_n\phi_n) = 0\ . \tag{6}$$

After multiplying all terms of equation (6) by R_n and combining the last two terms we obtain the desired model equation simulating angular oscillations of the n-the pendulum:

$$I_n\frac{d^2\phi_n}{dt^2} + m_n gR_n\sin(\phi_n) - KR_n(R_{n+1}\phi_{n+1} - 2R_n\phi_n + R_{n-1}\phi_{n-1}) = 0\ . \tag{7}$$

Returning to the case of DNA we will interpret the function $\phi_n(t)$ as the angular deviation of the n-th base, I_n and m_n – the moment of inertia and mass of the n-th base, R_n – the distance

from the center of mass of the *n*-th base to the sugar-phosphate chain, *K* – the rigidity of the sugar-phosphate chain. For DNA, equation (7) is written as:

$$I_n \frac{d^2\phi_n}{dt^2} + V_n \sin(\phi_n) - KR_n(R_{n+1}\phi_{n+1} - 2R_n\phi_n + R_{n-1}\phi_{n-1}) = 0\,, \tag{8}$$

where V_n is the coefficient characterizing interactions (hydrogen bonds) between the bases inside the *n*-th base pair.

In the continuum limit:

$$\begin{aligned} &a \to 0,\\ &z_n \to z,\\ &\phi_n(t) \equiv \phi(z_n,t) \to \phi(z,t),\\ &R_n \equiv R(z_n) \to R(z),\\ &I_n \equiv I(z_n) \to I(z),\\ &V_n \equiv V(z_n) \to V(z) \end{aligned} \tag{9}$$

model equation (8) becomes:

$$I(z)\frac{\partial^2\phi}{\partial t^2} + V(z)\sin\phi - KR(z)a^2\frac{\partial^2\left[R(z)\phi\right]}{\partial z^2} = 0\ . \tag{10}$$

The desired equation (10) can be written in a more convenient form:

$$I(z)\frac{\partial^2\phi}{\partial t^2} - K'(z)a^2\frac{\partial^2\phi}{\partial z^2} + V(z)\sin(\phi) - \frac{K'(z)a^2}{R(z)}\left[2\frac{\partial\phi}{\partial z}\frac{\partial R(z)}{\partial z} + \phi\frac{\partial^2 R(z)}{\partial z^2}\right] = 0\,. \tag{11}$$

The first three terms in equation (11) can be found in the old model equation – the sine-Gordon equation with the coefficients depending on the variable *z*:

$$I(z)\frac{\partial^2\phi}{\partial t^2} + V(z)\sin\phi - K'(z)a^2\frac{\partial^2\phi}{\partial z^2} = 0\ , \tag{12}$$

where $K'(z) = KR^2(z)$ is the torsion rigidity of the sugar-phosphate chain. The fourth term is a new additional correction, allowing take into account more accurately the heterogeneous nature of the DNA sequence.

Note that in the homogeneous case, the fourth term becomes zero, and Eq. (11) transforms to the classical sine-Gordon equation:

$$I\frac{\partial^2\phi}{\partial t^2} + V\sin\phi - K'a^2\frac{\partial^2\phi}{\partial z^2} = 0$$

with constant coefficients *I*, *V*, *K*' and *a*. The values of the parameters are presented in the Table 1.

Table 1. Parameters of homogeneous DNA sequences.

Sequence	*I* 10^{-44} [kg m^2]	*V* 10^{-20} [J]	*K*' 10^{-18} [J]	*R* 10^{-10} [m]	*a* 10^{-10} [m]
poly·(A)	7.61	2.09	2.27	5.8	3.4
poly·(T)	4.86	1.43	1.56	4.8	3.4
poly·(G)	8.22	3.12	2.20	5.7	3.4
poly·(C)	4.11	2.12	1.50	4.7	3.4

One-soliton solution of the sine-Gordon equation – kink – has the form

$$\phi(z,t) = 4\arctan\left(\exp\left(\frac{\gamma}{d}\left[z - vt - z_0\right]\right)\right)$$

where v is the velocity of kink, $\gamma = \left(1-\left(v/c_0\right)^2\right)^{1/2}$, $c_0 = \left(K'a^2/I\right)^{1/2}$ is the velocity of sound in DNA, $d = \left(K'a^2/V\right)^{1/2}$ is the size of kink, z_0 is arbitrary constant.

NUMERICAL SOLUTION OF THE MODEL EQUATION AND DNA KINK TRAJECTORIES

To solve the equation (11), let us take, as an example, artificial sequence consisting of two homogeneous regions: region 1 and region 2. Then the coefficients of the model equation (11) behave as follows: they are constant inside the homogeneous regions and they dramatically change near the boundary that separates the two regions. This behavior can be modeled with the help of σ-functions:

$$\begin{aligned} I(z) &= I_1 + \frac{I_2 - I_1}{1+\exp\left((z^*-z)/\sigma\right)}, \\ V(z) &= V_1 + \frac{V_2 - V_1}{1+\exp\left((z^*-z)/\sigma\right)}, \\ R(z) &= R_1 + \frac{R_2 - R_1}{1+\exp\left((z^*-z)/\sigma\right)}, \end{aligned} \qquad (13)$$

where I_i, V_i, R_i are the values of the coefficients within the homogeneous sections (i = 1, 2), z^* is the coordinate of the boundary, σ is an arbitrary parameter. When $\sigma \to 0$, the σ-functions (13) tend to the Heaviside step functions.

We solved numerically equation (11) with the coefficients (13), initial conditions

$$\phi(0,z) = 4\arctan\left(\exp\left(\frac{\gamma_1}{d_1}\left[z - z_0\right]\right)\right), \quad \frac{\partial}{\partial t}\phi(t,z)\Big|_{t=0} = -2v_0\frac{\gamma_1/d_1}{\cosh\left(\frac{\gamma_1}{d_1}\left[z - z_0\right]\right)}.$$

and conditions at the ends of the sequence:

$$\phi(t,-\infty) = 0, \ \phi(t,\infty) = 2\pi \ .$$

The kink-like solution $\phi(z,t)$ has been found with the help of the program «GRYZ» [11]. To study the kink behavior we constructed the kink trajectory. For this, we calculated the derivative $\partial\phi/\partial z$ which had the form of a ridge, and then we projected the top of the ridge on the plane (z,t). The calculations were made for the four artificial sequences (Fig. 2), which previously gave contradictory results [8]. For convenient carrying the computer experiment we selected the following lengths of the regions: the length of the first region was equal to 400 base pairs (*bp*) and the length of the second region – 200 *bp*. For definiteness, we assumed that at the initial time the kink began to move from the center of the first region with the velocity v = 400 *m*/*s*.

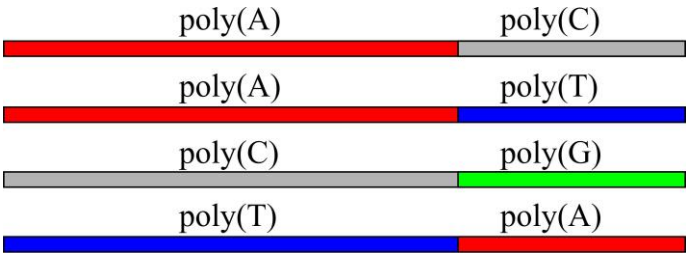

Fig. 2. Schematic picture of four artificial sequences having the length L = 600 *bp*.

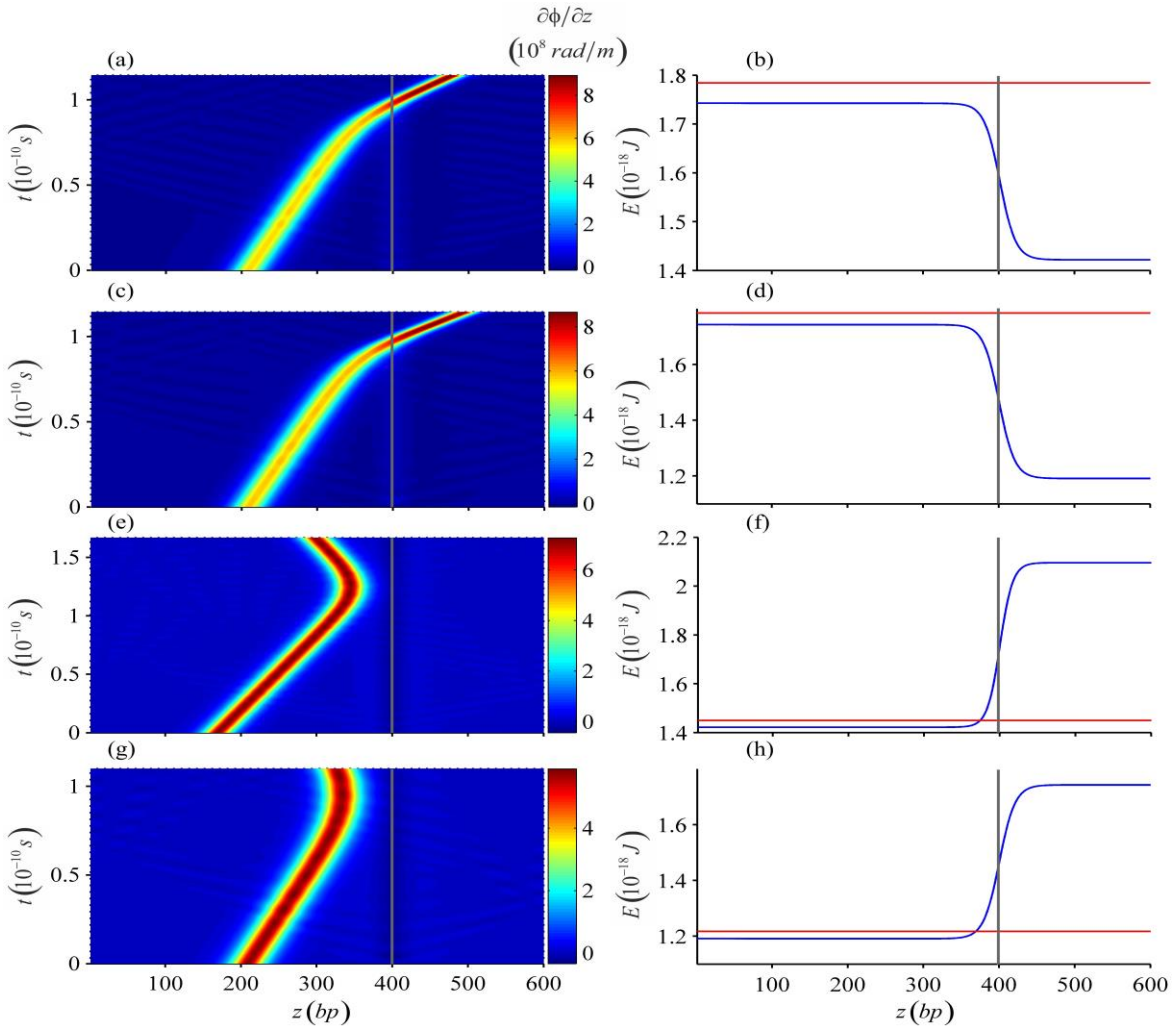

Fig. 3. Left – the trajectories of the kinks propagating in the artificial sequences: (a) poly(A) – poly(C), (c) poly(A) – poly(T), (e) poly(C) – poly(G), (g) poly(T) – poly(A). Right – the potential energy profiles of the sequences (blue curves) and total (kinetic and potential) energies of the kinks ((red lines) b), (d), (f), (h). The initial velocity of the kink v = 400 *m/s*. Vertical gray lines show the boundaries between homogeneous regions.

The results of numerical calculations are presented in Fig. 3. The kink trajectories are located in the left column. The potential energy profiles of the sequences which are determined by formula $E(z) = 8\sqrt{V(z)KR^2(z)}$, are located in the right column. The total energies of kinks (red lines) are constants because of the absence of dissipation in the considered model. It can be seen that kink overcomes the boundary separating two homogeneous regions in the first two sequences (Fig. 3, a, c), and the kink is reflected from the boundary in the other two sequences (Fig. 3, e, g).

This behavior of the kinks becomes clear from the energy profiles shown in Fig. 3, b, d, f, h. In the first two cases (Fig. 2, b, d) the total energy of the kink is large enough to cross the boundary. Moreover, the crossing of the boundary is accompanied by the increasing of the velocity of the kink. This is also to be expected, since in the absence of dissipation, the total kink energy must be conserved. So, a decrease of the potential energy of the kink to the right of the boundary leads an increase of the kinetic energy of the kink, and consequently, to an increase of kink velocity. In the other two sequences kinks reflect from the boundaries (Fig. 2, e, g). These results are also quite understandable. From Fig. 2, e, h one can see that the total energies of the kinks are not large enough to overcome the boundaries.

Thus, no contradictions in the behavior of the kink are observed. This indicates that the new model equation (11) more appropriately describes angular oscillations of the bases in heterogeneous DNA, compared with the old equation (12).

ZIGZAG SHAPED PERTURBATION OF THE KINK PROFILE NEAR THE BOUNDARY

When carrying out numerical calculations with the help of equation (11) we noticed unusual behavior of the function $\phi(z, t)$ near the boundary that separate homogeneous regions. To better examine the effect, let us increase the total length of the artificial sequence poly(A)–poly(C) (Fig. 4) from 600 till 1700 *bp* and suggest that that kink begins to move from the first region having the length 1000 *bp*.

Fig. 4. Schematic picture of artificial sequence poly(A)–poly(C).

The results of numerical calculations are presented in Fig. 5. The surface $\phi(z, t)$ is shown in Fig. 5,a. Ten cuts of the surface (profiles) at regular time intervals $\Delta t \approx 0.67 \times 10^{-10} s$ are shown in Fig. 5,b. The profile (1) corresponds to the initial condition which is the kink solution of the model equation (11) in the absence of any boundaries. Starting from the profile (2) the zigzag shaped perturbation of the kink profile near the boundary is clearly observed. This effect disappears at the cut (10) which corresponds to the profile of the kink after the crossing of the boundary. So, the "zigzag" is sitting motionless on the boundary and disappears only after the kink crosses the boundary.

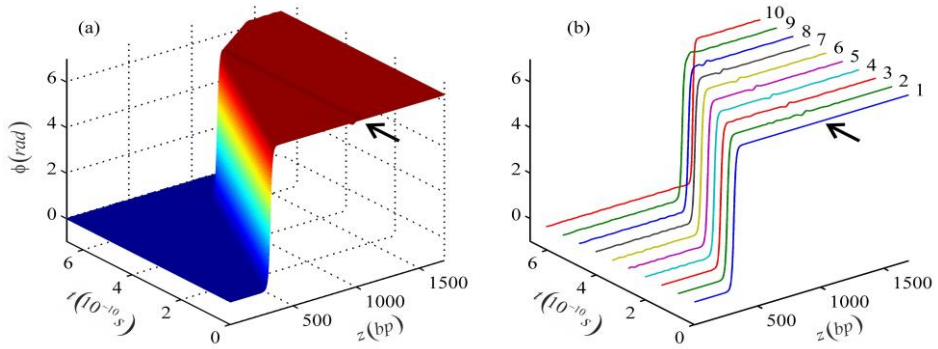

Fig. 5. (a) – kink propagating along artificial DNA sequence poly(A) – poly(C); (b) – 10 kink positions in time. The black arrows indicate the zigzag shaped perturbation near the boundary. The initial kink velocity $v = 400$ *m/s*.

To show that the zigzag effect is a consequence of modification of the model equation, we present in Fig. 6 the solution of the "old" model equation (12). It can be seen that there is not any zigzag effect. Moreover, we see that kink is reflected from the boundary. This behavior is in contradiction with physical sense because according to energetic profile (Fig. 3,b) there is not any energetic barrier which could prevent the kink movement.

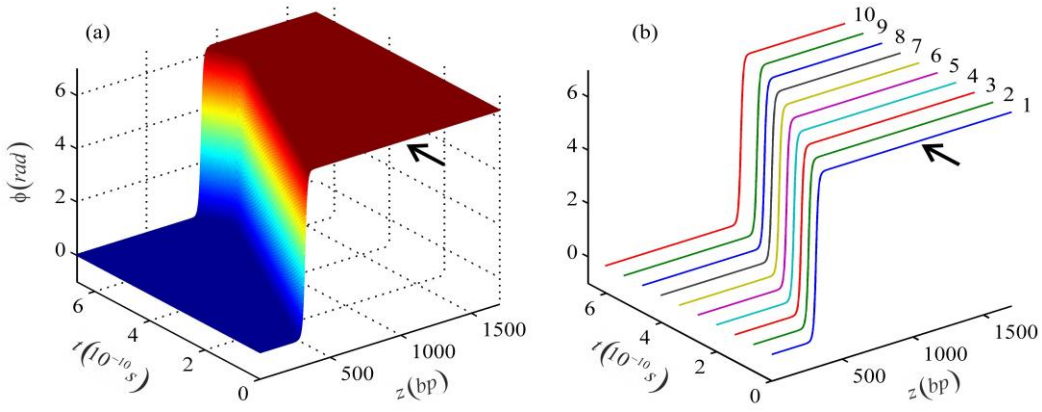

Fig. 6. (a) – solution of the "old" model equation (12) – kink propagating along artificial DNA sequence poly(A) – poly(C); (b) – 10 kink positions in time. The black arrows indicate the absence of the zigzag shaped perturbation near the boundary. The initial kink velocity $v = 400$ *m/s*.

To investigate the changes of the kink profile in more detail, we have increased the scale and showed in Fig. 7 the projections of the upper and the lower parts of the kink profiles on the plane (z, ϕ). It can be seen that the main effect (zigzag shaped perturbation) is clearly seen in all projections. It is also evident that the effect is only observed in the upper part of the profiles (Fig. 7,a) and is not observed in the lower part (Fig. 7,b). In addition to "zigzag", we see in Fig. 7 small fluctuations due perhaps to deficiencies of the numerical scheme. The increasing of the distance between the 9th and 10th cuts observed in Fig. 7, means increasing the velocity of the kink after passing the boundary.

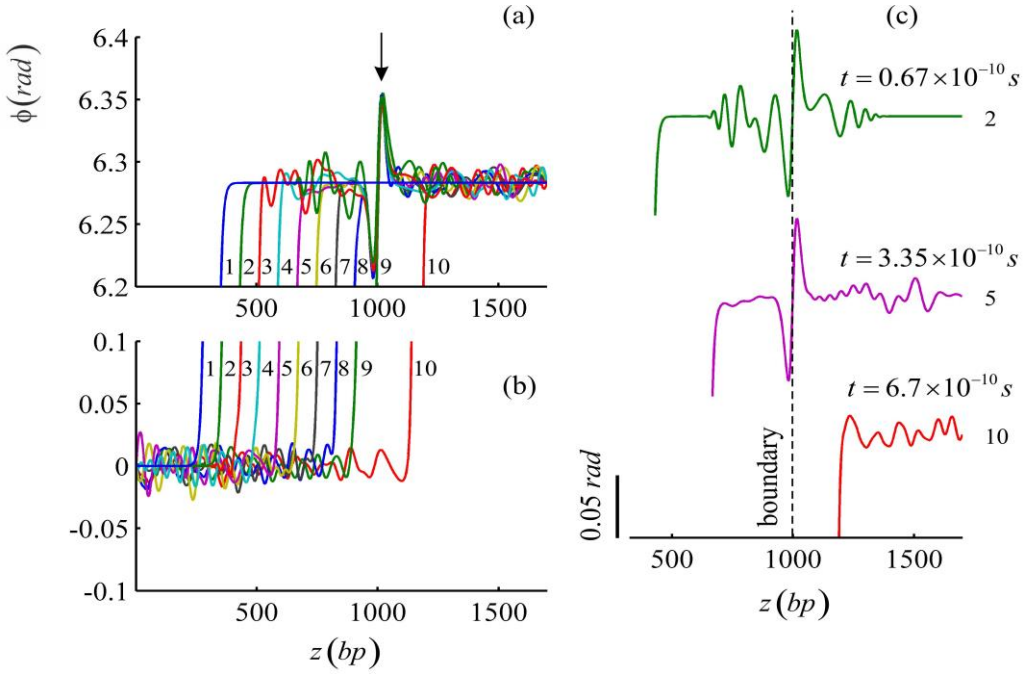

Fig. 7. Projections of the upper (a) and the lower (b) parts of the ten kink profiles on the plane (z, φ) are shown in the larger scale. The arrow indicates the zigzag shaped perturbation near the boundary. Upper parts of the three profiles (2, 5 and 10) are shown separately (c). The initial kink velocity $v = 400$ *m/s*. Parameter $\sigma = 1$.

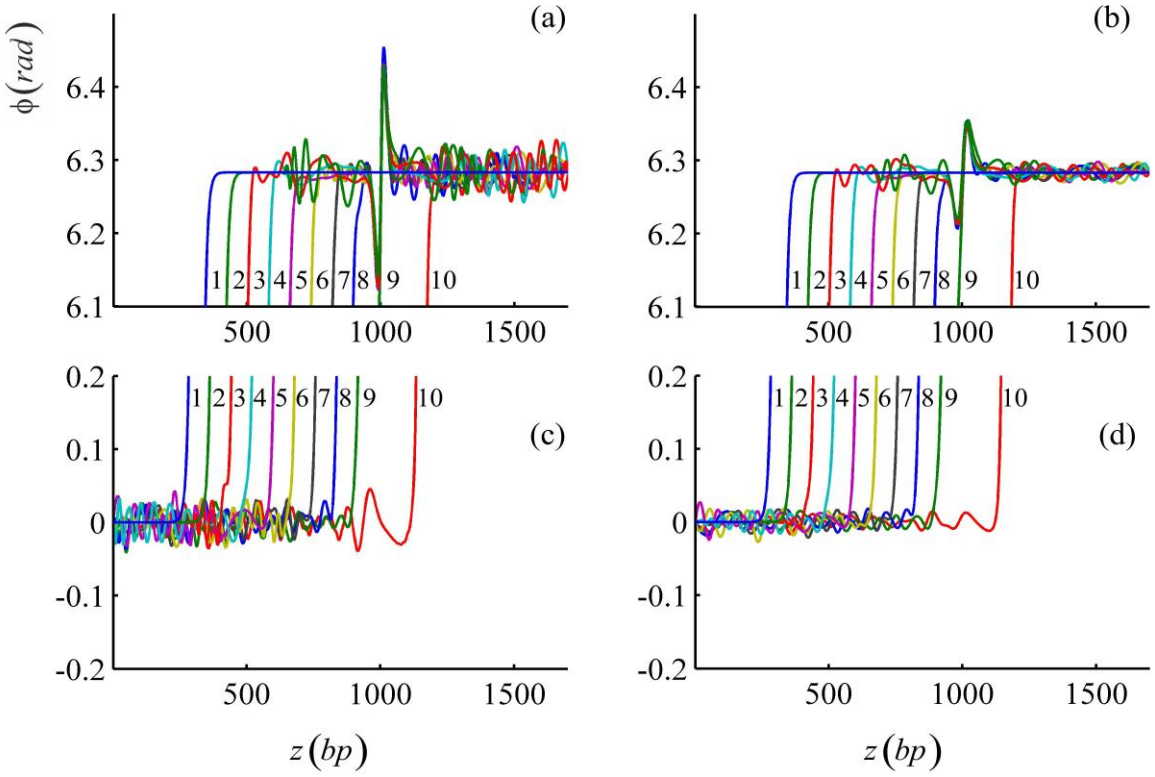

Fig. 8. Projections of the upper (a), (b) and lower (c), (d) parts of the ten kink profiles on the plane (*z*, φ) calculated for two different values of σ: $\sigma = 0.5$ (a), (c) and $\sigma = 1$ (b), (d). The initial kink velocity $v = 400$ *m/s*.

To study the dependence of the amplitude of the "zigzag" on the parameter σ, we calculated the projections of the upper and the lower parts of the kink profiles on the plane (*z*, φ) for two different values of σ: $\sigma = 0.5$ and $\sigma = 1$ (Fig. 8). The result was as follows: the larger σ, the smaller amplitude.

We also noticed that the zigzag perturbation was not symmetric with respect to the boundary. For example, in the case of sequence poly(A) – poly (C) (Fig. 4), the minimum of zigzag was located to the left of the boundary, and the maximum – to the right (Fig. 7,c). To check whether this arrangement of maxima and minima is conserved for the other sequences, we considered the opposite or "reverse" sequence (Fig. 9).

Fig. 9. Schematic picture of artificial sequence poly(C) – poly(A).

The result of numerical calculations of the solution $\phi(z,t)$ is presented in Fig. 10,a. In Fig. 10,b we show ten cuts of the surface (profiles) at regular time intervals $\Delta t \approx 0.67 \times 10^{-10}$ *s*. Projections of the upper and lower parts of the ten kink profiles on the plane (*z*, φ) are presented in Fig. 10,c, d. It can be seen that the form of zigzag has changed: Maximum became located to the left, and the minimum – to the right.

The energy profile of the sequence poly(A) – poly(C) has a "step down" form (Fig. 3,b). The energy profile of the opposite sequence poly(C) – poly(A) has obviously a "step up" form (or a barrier). Perhaps this explains the opposite locations of the zigzag maxima and minima in these two cases.

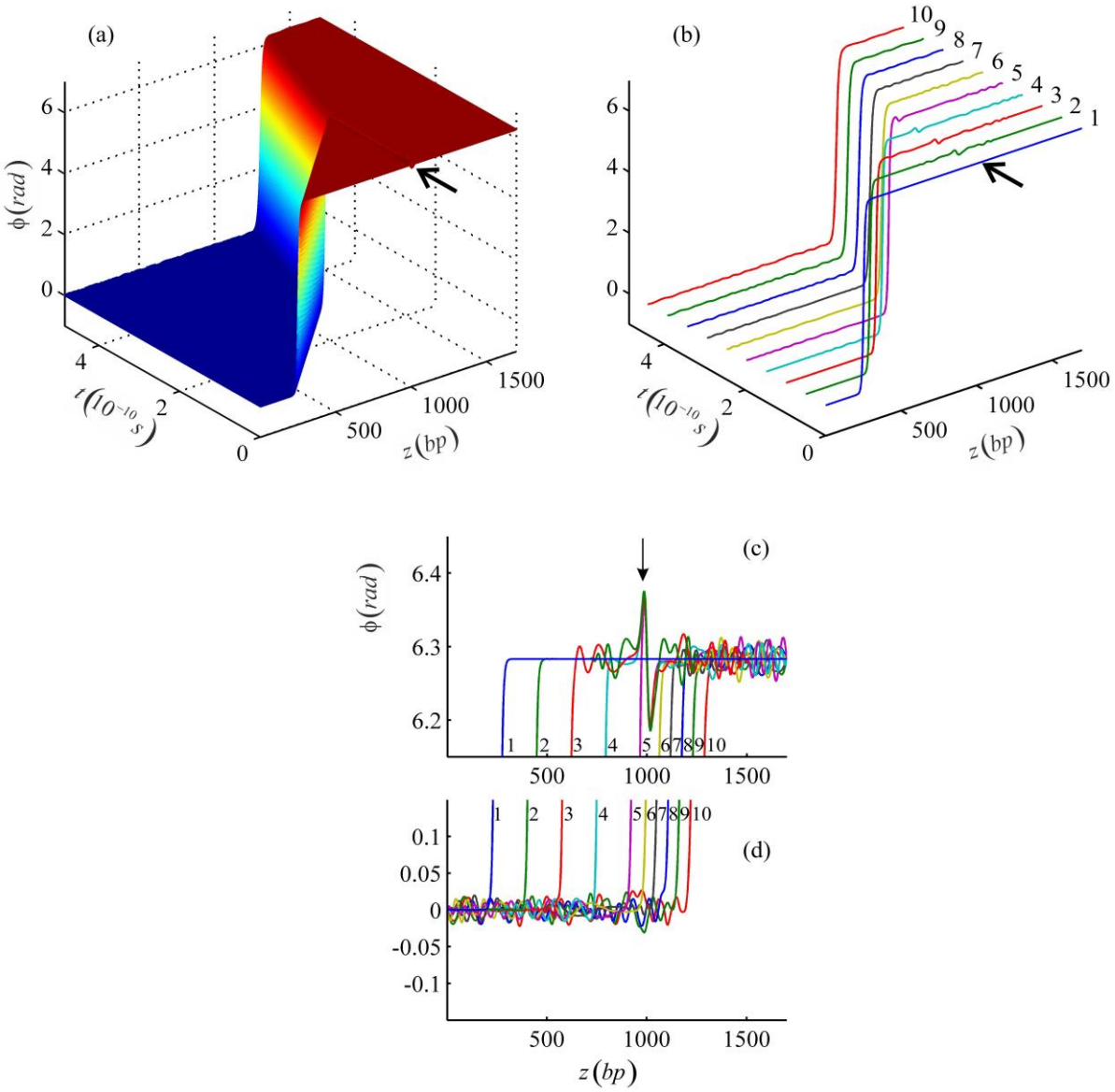

Fig. 10. (a) – kink propagating along artificial DNA sequence poly(C) – poly(A); (b) – 10 kink positions in time; projections of the upper (c) and lower (d) parts of the ten kink profiles on the plane (z, φ) shown in the larger scale. The black arrows indicate the "zigzag" change near the boundary. The initial kink velocity $v = 1200$ *m/s*. Parameter $\sigma = 1$.

KINK ENERGY DENSITY NEAR THE BOUNDARY

Taking into account the above results we can assume that the kink energy density should be also changed near the boundaries that separate homogeneous regions. To test this hypothesis, we constructed the Lagrangian and Hamiltonian corresponding to the new model equation (11). Generally speaking, methods of constructing the Lagrangian and Hamiltonian may be different (see Appendix). Here we apply the method that is commonly used in solid-state theory. For the purpose, let us write firstly the Lagrangian and Hamiltonian for the discrete equation (8):

$$L = \sum_n \left[\frac{I_n \left(\frac{d\phi_n}{dt} \right)^2}{2} - V_n (1 - \cos(\phi_n)) - \frac{K \left(R_n \phi_n - R_{n-1} \phi_{n-1} \right)^2}{2} \right], \qquad (14)$$

$$H=\sum_n\left[\frac{I_n\left(\frac{d\phi_n}{dt}\right)^2}{2}+V_n(1-\cos\phi_n)+\frac{K\left(R_n\phi_n-R_{n-1}\phi_{n-1}\right)^2}{2}\right]. \quad (15)$$

After that let us pass to the continuum limit:

$$L=\int\left[\frac{I(z)}{2}\left(\frac{\partial\phi}{\partial t}\right)^2-V(z)(1-\cos\phi)-\frac{Ka^2}{2}\left(\frac{\partial(R(z)\phi)}{\partial z}\right)^2\right]\frac{dz}{a}, \quad (16)$$

$$H=\int\left[\frac{I(z)}{2}\left(\frac{\partial\phi}{\partial t}\right)^2+V(z)(1-\cos\phi)+\frac{Ka^2}{2}\left(\frac{\partial(R(z)\phi)}{\partial z}\right)^2\right]\frac{dz}{a}. \quad (17)$$

Then the Lagrangian density (the integrand in (16)) can be written as follows:

$$\rho_L=\frac{I(z)}{2}\left(\frac{\partial\phi}{\partial t}\right)^2-V(z)(1-\cos\phi)-\frac{KR^2(z)a^2}{2}\left(\frac{\partial\phi}{\partial z}\right)^2-\frac{Ka^2}{2}\left[\phi^2\left(\frac{dR}{dz}\right)^2+\phi\frac{\partial\phi}{\partial z}\frac{d^2(R^2)}{dz^2}\right]. \quad (18)$$

Similarly, we can write the Hamiltonian density (or energy density):

$$\rho_H=\frac{I(z)}{2}\left(\frac{\partial\phi}{\partial t}\right)^2+V(z)(1-\cos\phi)+\frac{KR^2(z)a^2}{2}\left(\frac{\partial\phi}{\partial z}\right)^2+\frac{Ka^2}{2}\left[\phi^2\left(\frac{dR}{dz}\right)^2+\phi\frac{\partial\phi}{\partial z}\frac{d^2(R^2)}{dz^2}\right]. \quad (19)$$

Formulas (18) and (19) consist of two parts. The first part contains the first three terms and corresponds to the old model equation (12). The second part corresponds to the fourth term in the new model equation (11). This part is an additional correction which allows take into account more accurately the heterogeneous nature of the DNA sequence.

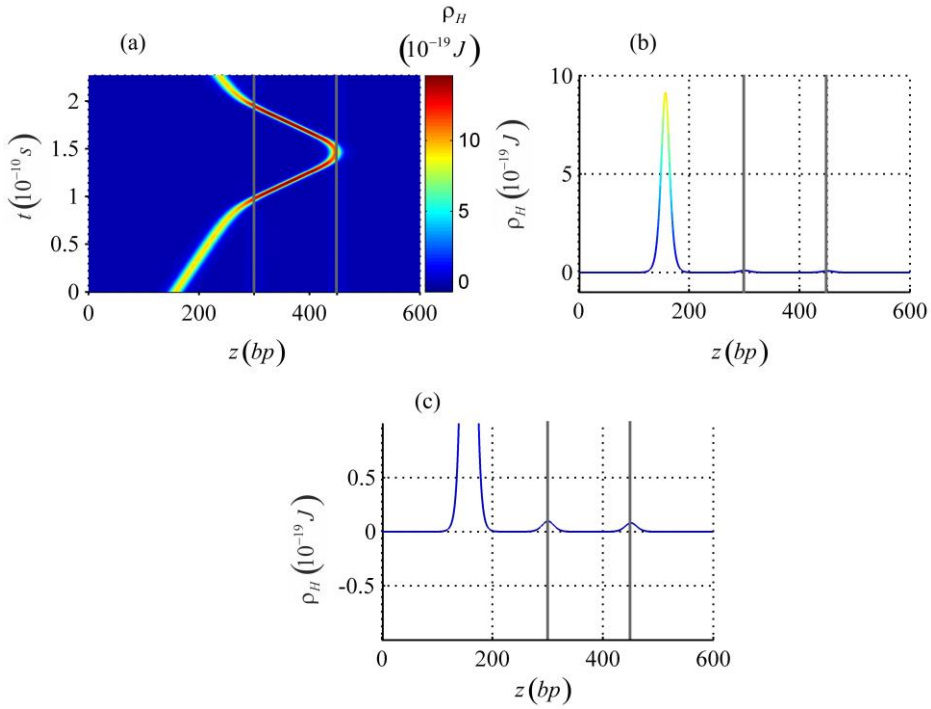

Fig. 11. Projections of the kink energy density $\rho_H(z,t)$ on the plane (z,t) (a) and on the plane (z,ρ_H) (b) in a narrow time interval $t=[0,\ 2.27]$ $(10^{-15}\ s)$ near the start point of the kink movement. The same projection on the plane (z,ρ_H), but in a larger scale. The initial kink velocity $v=400$ *m/s*. Vertical gray lines indicate the boundaries between homogeneous regions.

Fig. 11 shows the results of calculating the energy density for the case of a sequence consisting of three homogeneous regions: poly(A), poly(C) and poly(G). The length of the first region is 300 *bp*, the length of the second region – 150 *bp*, and the length of the third – 150 *bp*. The projections of the kink energy on the planes (z, t) and (z, ρ_H) are presented in Fig. 11a, b. We can see that small bell-shaped perturbations of the kink energy density are actually observed near the boundaries. In Fig. 11,c we used a larger scale to show the perturbations more clearly.

CONCLUSIONS AND DISCUSSION

In this paper a new version of the model equation simulating angular oscillations of the nitrous bases in heterogeneous DNA has been presented. Numerical solutions in the form of kinks have been obtained for the sequences consisting of two or more homogeneous regions separating by boundaries. Trajectories of the kinks moving in the sequences have been constructed. It was shown that contradictions in the kinks behavior observed earlier in the frameworks of the old model have been overcome.

The new model equation was applied to study the behavior of kinks near the boundaries separating the homogeneous regions of DNA. We found the zigzag perturbations of the kink profiles near the boundaries and investigated their properties in detail.

Mechanistic interpretation of the obtained results is shown in Fig. 12.

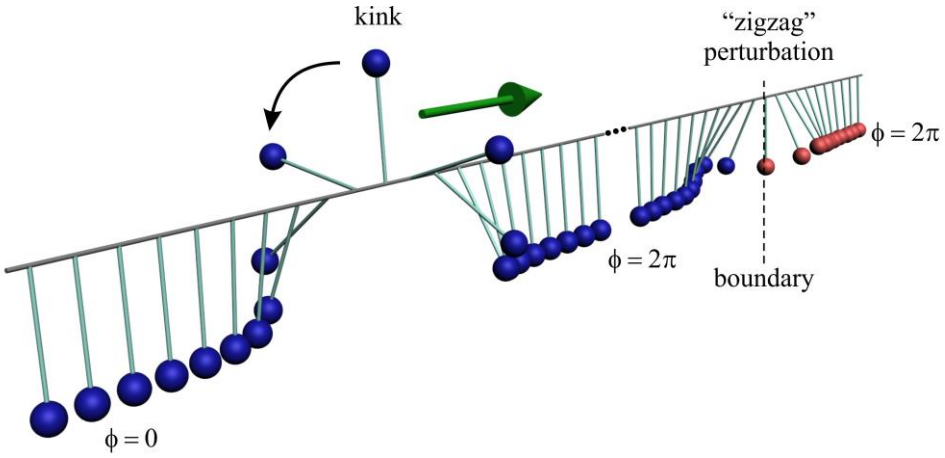

Fig. 12. Kink and zigzag perturbation in the mechanical model. Zigzag perturbation is shown on a larger scale. Green arrow indicates the direction of kink movement, black arrow – the direction of rotation.

We showed that the amplitude of the zigzag perturbation depended on the parameter σ. It was shown also that the energy density of the kink was undergoing a small perturbation near the boundaries. But in contrast to the zigzag-shaped perturbations of the kink profile, the energy density perturbations are bell-shaped.

The obtained numerical results could help in analytical studies of the new model. In particular, they point out that in the search for analytical solutions of the equation, it is quite correct to use perturbation theory, because perturbations observed in computer experiments are sufficiently small. They also prompt in what form to search these perturbations and what dynamic properties they should have.

APPENDIX

Let us write equation (11) in the form:

$$I(z)\frac{\partial^2\phi}{\partial t^2}-K'(z)a^2\frac{\partial^2\phi}{\partial z^2}+V(z)\sin(\phi)-\frac{K'(z)a^2}{R(z)}\left[2\frac{\partial\phi}{\partial z}\frac{\partial R(z)}{\partial z}+\phi\frac{\partial^2 R(z)}{\partial z^2}\right]=0, \quad \text{(A-1)}$$

where $K'(z)=KR^2(z)$.

In the field theory in 2-dimensional space-time, equations of motion are obtained from the Lagrangian as follows:

$$\partial_\mu\left(\frac{\partial L}{\partial(\partial_\mu\phi)}\right)-\frac{\partial L}{\partial\phi}=0, \quad \text{(A-2)}$$

where $\partial_\mu=(\partial_t,\partial_z)$. In (A-2) summation goes in the variable μ.

Let us group the terms in (A-1) in the derivatives of ϕ:

$$I\partial_{tt}\phi-a^2K'\partial_{zz}\phi-2a^2\frac{K'}{R}\partial_z R\partial_z\phi+V\sin(\phi)-a^2\frac{K'}{R}\partial_{zz}(R)\phi=0. \quad \text{(A-3)}$$

Next, we need to insert the coefficients from the expression $I\partial_{tt}\phi-a^2K'\partial_{zz}\phi$ into the first derivative and take into account that these coefficients depend on *z*. In the first term, it is trivially: $I\partial_{tt}\phi=\partial_t(I\partial_t\phi)$. In the second term, it is a bit more complicated. Take into account that $K'=K(R(z))^2$, where *K* is a constant. Then we have:

$$\begin{aligned}-a^2K'\partial_{zz}\phi&=-a^2KR^2\partial_{zz}\phi=-a^2K\left[\partial_z\left(R^2\partial_z\phi\right)-\partial_z\left(R^2\right)\partial_z\phi\right]=\\&=-a^2K\left[\partial_z\left(R^2\partial_z\phi\right)-2R\partial_z R\partial_z\phi\right].\end{aligned} \quad \text{(A-4)}$$

Inserting (A-4) into (A-3) we obtain:

$$\partial_t(I\partial_t\phi)-a^2K\left[\partial_z\left(R^2\partial_z\phi\right)-2R\partial_z R\partial_z\phi\right]-2a^2KR\partial_z R\partial_z\phi+V\sin(\phi)-a^2\frac{K'}{R}\partial_{zz}(R)\phi=0.$$

Or:

$$\partial_t(I\partial_t\phi)-\partial_z\left(a^2KR^2\partial_z\phi\right)+V\sin(\phi)-a^2\frac{K'}{R}\partial_{zz}(R)\phi=0.$$

Thus, we have:

$$\partial_t\left(\frac{\partial L}{\partial(\partial_t\phi)}\right)+\partial_z\left(\frac{\partial L}{\partial(\partial_z\phi)}\right)=\partial_t(I\partial_t\phi)+\partial_z\left(-a^2K'\partial_z\phi\right),$$

$$-\frac{\partial L}{\partial\phi}=V\sin(\phi)-a^2\frac{K'}{R}\partial_{zz}(R)\phi.$$

Hence it is easy to obtain:

$$L_t=I(z)\frac{(\partial_t\phi)^2}{2},\quad L_z=-a^2K'(z)\frac{(\partial_z\phi)^2}{2},$$

$$U=U_0+V(z)\cos(\phi)+a^2\frac{K'(z)}{R(z)}\partial_{zz}(R)\frac{\phi^2}{2}.$$

It follows from the condition $U=0$ at $\phi=0$ that $U_0=-V(z)$. Taking into account that $L=\int\left(L_t+L_z+U\right)\frac{dz}{a}$, we obtain finally:

$$L=\int\left[I(z)\frac{\left(\partial_t\phi\right)^2}{2}-a^2K'(z)\frac{\left(\partial_z\phi\right)^2}{2}-V(z)\left(1-\cos(\phi)\right)+a^2\frac{K'(z)}{R(z)}\frac{\phi^2}{2}\partial_{zz}(R)\right]\frac{dz}{a} \quad \text{(A-5)}$$

and therefore, the energy density of the kink is:

$$\rho_H^1=\frac{I(z)}{2}\left(\frac{\partial\phi}{\partial t}\right)^2+\frac{KR^2(z)a^2}{2}\left(\frac{\partial\phi}{\partial z}\right)^2+V(z)(1-\cos\phi)-a^2\frac{K'(z)}{R(z)}\frac{\phi^2}{2}\frac{\partial^2R}{\partial z^2}. \quad \text{(A-6)}$$

It is easy to show that formula (A-6) coincides with formula (19) (up to a total derivative). To prove this, it is sufficient to show the coincidence of the last terms. To do this, let us write the third term in (17) as follows:

$$\begin{aligned}&\frac{Ka^2}{2}\left(\frac{\partial(R(z)\phi)}{\partial z}\right)^2=\\&=\frac{Ka^2}{2}\left(R(z)\right)^2\left(\frac{\partial\phi}{\partial z}\right)^2+\frac{Ka^2}{2}\left[\left(\frac{\partial(\phi^2)}{\partial z}\right)\left(R(z)\frac{d(R(z))}{dz}\right)+\phi^2\left(\frac{d(R(z))}{dz}\right)^2\right].\end{aligned} \quad \text{(A-7)}$$

Next, rewrite (A-7) in a simpler form:

$$\frac{Ka^2}{2}R^2\phi_z^2+\frac{Ka^2}{2}\left[\left(\phi^2\right)_z\left(RR_z\right)+\left(\phi\right)^2\left(R_z\right)^2\right]. \quad \text{(A-8)}$$

Take into account that

$$\frac{\partial}{\partial z}\left[\left(\phi^2\right)\left(RR_z\right)\right]=\left(\phi^2\right)_z\left(RR_z\right)+\left(\phi\right)^2\left(R_z\right)^2+\left(\phi^2\right)\left(RR_{zz}\right). \quad \text{(A-9)}$$

Then instead of (A-8) we obtain:

$$\frac{Ka^2}{2}R^2\phi_z^2+\frac{Ka^2}{2}\left[\frac{\partial}{\partial z}\left[\left(\phi^2\right)\left(RR_z\right)\right]-\left(\phi^2\right)\left(RR_{zz}\right)\right].$$

REFERENCES

1. Englander S.W., Kallenbach N.R., Heeger A.J., Krumhansl J.A., Litwin S. Nature of the open state in long polynucleotide double helices: possibility of soliton excitations. *Proc. Natl. Acad. Sci. USA.* 1980. V. 77. P. 7222–7226.
2. Yakushevich L.V., Ryasik A.A. Dynamical characteristics of DNA kinks and antikinks. *Computer research investigations and modeling*. 2012. V. 4. № 1. P. 209–217.
3. Yakushevich L.V., Krasnobaeva L.A., Shapovalov A.V., Quintero N.R. One- and two-soliton solutions for DNA. *Biofizika*. 2005. V. 50. P. 450–455.
4. Salerno M. Discrete model for DNA-promoter dynamics. *Phys. Rev. A.* 1991. V. 44. P. 5292–5297. doi: 10.1103/PhysRevA.44.5292.
5. Lennholm E., Hornquist M. Revisiting Salernos sine-Gordon model of DNA: active regions and robustness. *Physica D: Nonlinear Phenomena*. 2003. V. 177. P. 233–241. doi: 0.1016/S0167-2789(02)00769-8.
6. Cuenda S., Sanchez A. Nonlinear excitations in DNA: Aperiodic models versus actual genome sequences. *Phys. Rev. E.* 2004. V. 70. № 5. P. 051903. doi: 10.1103/PhysRevE.70.051903.
7. Yakushevich L.V., Krasnobaeva L.A. A new approach to studies of non-linear dynamics of kinks activated in inhomogeneous polynucleotide chains. *Int. J. Nonl. Mech*. 2008. V. 43. P. 1074–1081.
8. Grinevich A.A., Ryasik A.A., Yakushevich L.V. The dynamics of polynucleotide chain consisting of two different homogeneous sequences, divided by interface. *Computer research and modeling*. 2013. V. 5. № 2. P. 241–254.
9. Grinevich A.A., Ryasik A.A., Yakushevich L.V. Trajectories of kinks movement in inhomogeneous potential field of DNA. In: *V International Conference on Mathematical Biology and Bioinformatics*: Proceedings of the Conference ICMBB5, 2010, Pushchino, Russia. Moscow: MAKS Press, 2014. P. 34-35.
10. Scott A.J. A nonlinear Klein-Gordon equation. *Am. Phys*. 1969. V. 37. P. 52–61.
11. Grinevich A.A., Ryasik A.A., Yakushevich L.V, Zakiryaniv F.K. *Numerical modeling of nonlinear conformation waves in inhomogeneous sequences of DNA*: certificate of registration of the computer program № 2014616737. Russian Federal Service for Intellectual Property (Rospatent), 2014.

Received March 25, 2015.
Published April 17, 2015.